

# A Polarization Insensitive Tri-Band Bandpass Frequency Selective Surface for Wi-MAX and WLAN Applications

Sanjeev Yadav<sup>1, \*</sup>, Mahendra M. Sharma<sup>2</sup>, and Rajesh K. Singh<sup>3</sup>

**Abstract**—This article reports a single layer tri-band bandpass, polarization insensitive Frequency Selective Surface (FSS). The unit cell is designed by considering different square loop elements and cross dipole element to pass Wi-Max and WLAN frequency range with low loss. Three different shapes of loops and one cross dipole are arranged in a way that gives a triple-band-pass characteristic from the proposed structure. These loops and dipole are designed to pass Wi-MAX (2.5–2.7 GHz, 3.4–3.6 GHz) and WLAN (center frequency, 5.5 GHz) bands. The structure performance is independent of incidence angle of wave due to its symmetrical geometry which makes the design polarization insensitive and achieves good angular stability. A  $14 \times 14$  array of proposed unit cell is realized and measured. The proposed FSS achieves a 3 dB transmission bandwidth of 25% at 2.6 GHz, 65.6% at 3.5 GHz, and 65.6% at 5.5 GHz. The advantage of the proposed design is that it has a simple and compact geometry fabricated on a low-cost substrate and achieved tri-band band pass response with a wide angular stability.

## 1. INTRODUCTION

Frequency Selective Surface (FSS) consists of identical metallic patches etched over a dielectric substrate periodically arranged in a two-dimensional array. These structures resonate at a specific frequency determined by their equivalent capacitance and inductance. These structures selectively reflect or transmit the frequency incident on the surface. Due to their selective property, frequency selective surfaces are used extensively for various applications, for instance, wireless security, reflectors, electromagnetic shielding, absorbers, and many more [1–4]. Periodic structures are also known as High Impedance Surfaces (HIS) [1]. Munk introduced the concept of periodic structure that can work as a frequency tuner: frequencies may be reflected, transmitted, and absorbed [2]. FSS has become an interesting research topic due to its comprehensive applications, such as hybrid radomes, band-stop filters, Dichroic sub-reflector, Dichroic main-reflector, circuit analog absorber, and meander line polarizer [2, 3].

The filtering property of FSS is not only the function of frequency, but also a function of incidence angle which makes the FSS more reliable and useful compared to a traditional microwave filter. Therefore, it is needed that an FSS provides a stable performance at various incidence angles and different polarization states within its operating range [2–6]. It can act as band pass radomes for missiles and can be used for enhancing the impedance bandwidth of the antenna [4–9, 14]. Multi-band characteristic of FSS plays a key role in deep space exploration [10]. Periodic structures can be simulated with the help of full wave electromagnetic (EM) solvers [11], but they can also be analyzed numerically using several approaches, such as equivalent circuit, spectral domain, vector-spectral domain, finite

---

*Received 11 September 2021, Accepted 27 November 2021, Scheduled 20 December 2021*

\* Corresponding author: Sanjeev Yadav (sanjeev.mnit@gmail.com).

<sup>1</sup> Department of Electronics and Communication Engineering, Govt. Women Engineering College, Ajmer 305002, India.

<sup>2</sup> Department of Electronics and Communication Engineering, Malaviya National Institute of Technology, Jaipur 302017, India.

<sup>3</sup> Department of Information Engineering, University of Pisa, Italy.

element, finite difference time domain, T-matrix, and many more [12]. Both finite [13] and infinite arrays can be considered for the analysis, but to save computation time, finite arrays can be taken.

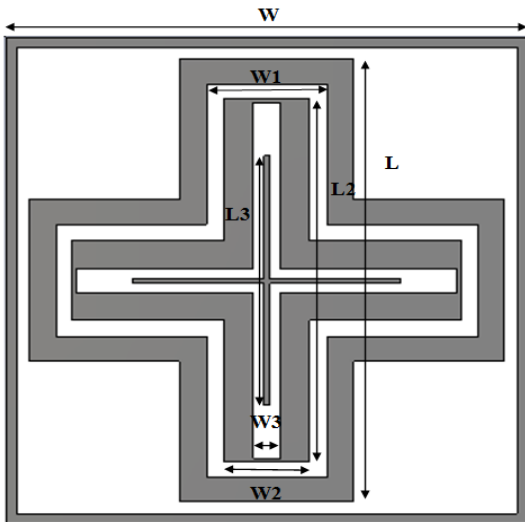
To get angular stability with respect to the incidence angle, a compact structure is required, and to get polarization insensitive behavior, a symmetrical geometry is required [15–19]. Several techniques have been reported in the scientific literature for realizing a multiband FSS from a single-band FSS. In several reported multiband FSS, the unit cell size was large as compared to the wavelength [11] while a few reported structures were multilayered with complex geometries, and they limit the angular stability [17].

In this article, it is tried to overcome the issues of complex geometry, poor angular stability, and large size. A compact, single layer tri-band bandpass, polarization insensitive FSS is proposed. The aim of the design is to pass frequencies lying in Wi-Max and WLAN bands with low insertion loss. These three passbands are obtained by arranging three different loops and a cross dipole. The dimensions of the loops are adjusted in such a way that low insertion loss is achieved at the desired frequency bands. The proposed FSS is designed, fabricated, and measured. The results obtained by means of simulation, measurement, and equivalent circuit approach are plotted and compared. The article is organized in the following order. The design and analysis of unit cell are discussed in Section 2. Equivalent circuit model is derived in Section 3. Performance of the FSS in terms of  $S$ -parameters is discussed in Section 4. Finally, the article is concluded in Section 5.

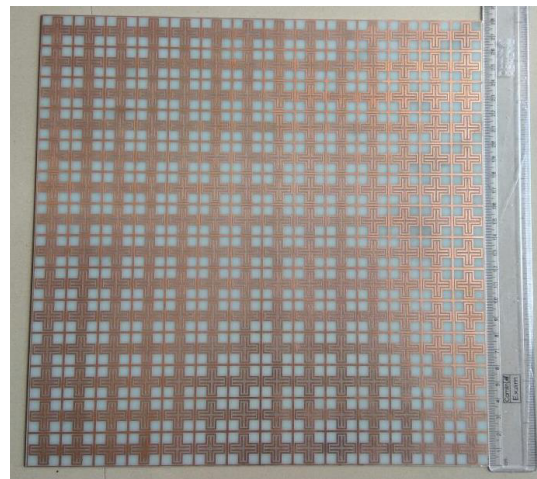
## 2. DESIGN AND ANALYSIS OF UNIT CELL

Figure 1 illustrates the geometry of the proposed unit cell. To achieve the tri-band characteristic, three different loops along with a cross dipole are utilized. The dimensions of the loops and spacing between the loops are adjusted to get the desired performance. The unit cell is realized on a 1.6 mm thick FR4 substrate with dielectric constant of 4.4. The dimension of unit cell is  $0.16\lambda \times 0.16\lambda$ , where  $\lambda$  corresponds to the wavelength of first resonant frequency.

The design of a compact and stable FSS to be operated at lower frequencies is slightly difficult. In order to possess insensitivity towards polarization, symmetrical structure is needed. Therefore, a symmetrical metallic square loop has been introduced to achieve the lower operating frequency and miniaturized design as well. The lowest frequency band, i.e., 2.5–2.7 GHz, is achieved which corresponds to the outer square loop. To obtain the second frequency band, i.e., 3.4–3.6 GHz, two plus-shaped loops are etched. The third frequency band, i.e., 5.2–5.8 GHz, is achieved by etching a cross dipole in the centre of the unit cell. The optimized dimensions of the unit cell are listed in Table 1.



**Figure 1.** Geometry of a single unit cell.



**Figure 2.** Fabricated FSS by realizing an array of  $14 \times 14$  unit cells.

**Table 1.** Dimensions of the proposed unit cell.

Name of Dimension	Symbol	Value (in mm)
Height of the substrate	$H$	1.6
Width of substrate and outer loop	$W$	19.5
Length of outer loop	$L$	17.8
Width of outer plus-shaped loop	$W1$	4.5
Length of inner plus-shaped loop	$L2$	14.6
Width of inner plus-shaped loop	$W2$	3.2
Width of inner cross dipole	$W3$	1.0
Length of inner cross dipole	$L3$	10

FSS is designed by making an array of proposed unit cell in CST Microwave Studio using frequency domain solver, and Floquet port analysis is done for TE and TM modes. A  $14 \times 14$  array with a size of  $273 \text{ mm} \times 273 \text{ mm}$  is fabricated through a chemical etching process as shown in Fig. 2.

### 3. EQUIVALENT CIRCUIT MODEL ANALYSIS

When the plane wave is obliquely incident on the metallic surface of FSS, the electrons on the metal surface starts oscillating, and the current gets induced in the loops. These loops behave as electrical components, and an equivalent circuit is derived for the proposed unit cell as shown in Fig. 3. The metallic closed loop of the unit cell acts as inductance, and the spacing between the loops acts as the capacitance. These inductances and capacitances are realized by properly arranging the loops to get desired passband response. Three parallel LC resonant circuits represent three passbands as shown in Fig. 3.

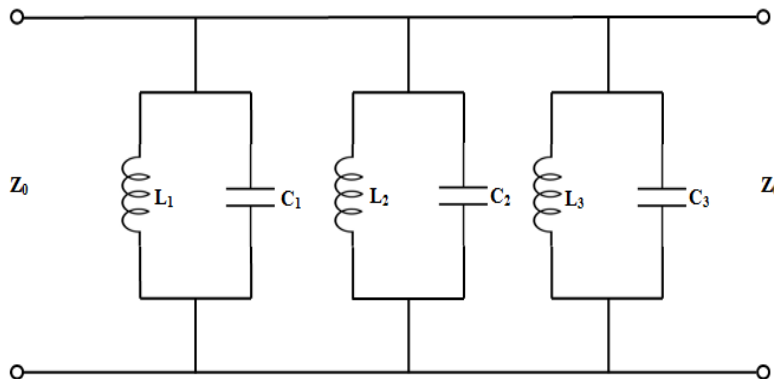


**Figure 3.** Equivalent-circuit model of a unit cell.

The equivalent-circuit model of proposed unit cell is derived and the response evaluated mathematically. This equivalent model is applicable to normal incidence of plane wave.

The values of lumped elements  $L_1, L_2, L_3$  and  $C_1, C_2, C_3$  can be calculated from Eqs. (1) and (2) [1]:

$$C = \epsilon_0 \epsilon_{eff} \frac{2p}{\pi} \ln \left[ \frac{1}{\sin \left( \frac{\pi d}{2p} \right)} \right] \tag{1}$$

$$L = \mu_0 \mu_{eff} \frac{l}{2\pi} \ln \left[ \frac{1}{\sin \left( \frac{\pi w}{2l} \right)} \right] \quad (2)$$

In above equations,  $C$  is the capacitance,  $\epsilon_0$  the free space permittivity,  $\epsilon_{eff}$  the effective relative permittivity,  $p$  (where  $p = l = D - w - s$ ) the periodicity,  $D$  the size of the element,  $s$  (where  $2d = s$ ) the space between elements,  $w$  the width of the element,  $L$  the inductance,  $\mu_0$  the free space permeability, and  $\mu_{eff}$  the effective relative permeability.

Individual inductance and capacitance are calculated from Equations (1) & (2). Based on these inductance and capacitance values resonant frequencies are calculated from Equation (3), and  $f_r$  is the resonating frequency of the particular passband.

$$f_r = \frac{1}{2\pi\sqrt{LC}} \quad (3)$$

The calculated values from above equations are illustrated in Table 2.

**Table 2.** Dimensions and values of the equivalent circuit of proposed unit cell.

	$D$ (mm)	$w$ (mm)	$s$ (mm)	$p$ (mm)	$d$ (mm)	$L$ (nH/mm)	$C$ (pF/mm)	$f_r$ (GHz)
Outer ring	19.5	0.8	0.5	18.2	0.3	6.89	0.591	2.49
Middle ring	17.8	1.0	0.9	15.9	0.4	5.19	0.415	3.4
Inner ring	14.3	1.0	1.6	12.0	0.8	3.54	0.226	5.6

Using these parameter values, circuit simulations have been performed with Advance System Design (ADS) simulation tool to verify the model.

## 4. RESULTS AND DISCUSSION

### 4.1. Simulated Results

The proposed unit cell has been modelled and analysed using the Floquet port over the required frequency ranges. Transmission response is achieved for the Transverse Electric (TE) and Transverse Magnetic (TM) modes as plotted in Fig. 4. It is observed that three passbands at center frequencies of 2.5 GHz, 3.5 GHz, and 5.5 GHz are achieved. Insertion loss of 0.32 dB, 1.18 dB, and 0.76 dB has been achieved in the first, second, and third operating bands, respectively, and rest of the frequencies are reflected back.

Similarly, reflection performance has been obtained. Reflection coefficient of  $-34$  dB,  $-19$  dB, and  $-33$  dB has been achieved at the first, second, and third operating bands, respectively. Reflection coefficients are plotted for TE and TM modes in Fig. 5.

The outer square loop is responsible for the lowest frequency band, 2.5 GHz, which is the desired lowest frequency band. The electric current flows on the perimeter of the outer square loop as illustrated in Fig. 6(a). The metallic part of two inner plus-shaped loops acts as inductance and spacing between them acts as capacitance, and their combination is responsible for the resonance at 3.5 GHz. The maximum current flows on the periphery of outer and inner plus-shaped loops as illustrated in Fig. 6(b), the metallic cross dipole operates at 5.5 GHz band. The current flows on the periphery of cross dipole as illustrated in Fig. 6(c).

### 4.2. Experimental Setup and Fabrication

The proposed FSS array of  $14 \times 14$  unit cells is fabricated as shown in Fig. 2. To measure the performance, the fabricated FSS is placed between two identical wideband double-ridged horn antennas surrounded by absorbers as illustrated in Fig. 7.

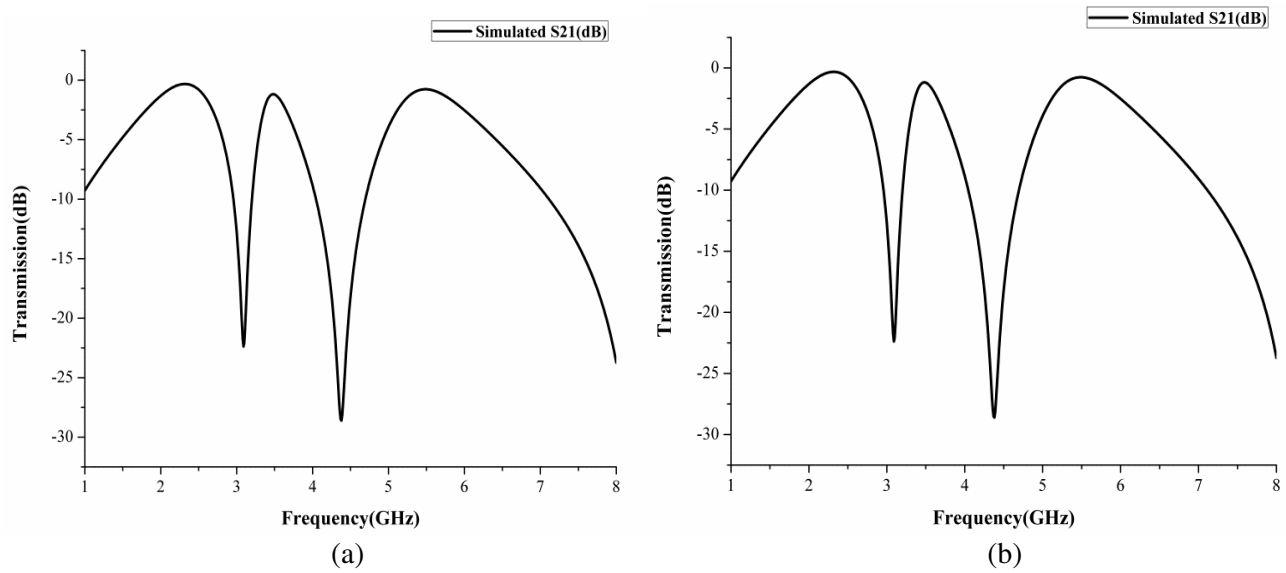


**Figure 4.** Simulated transmission coefficient of proposed unit cell for (a) TE mode, (b) TM mode.

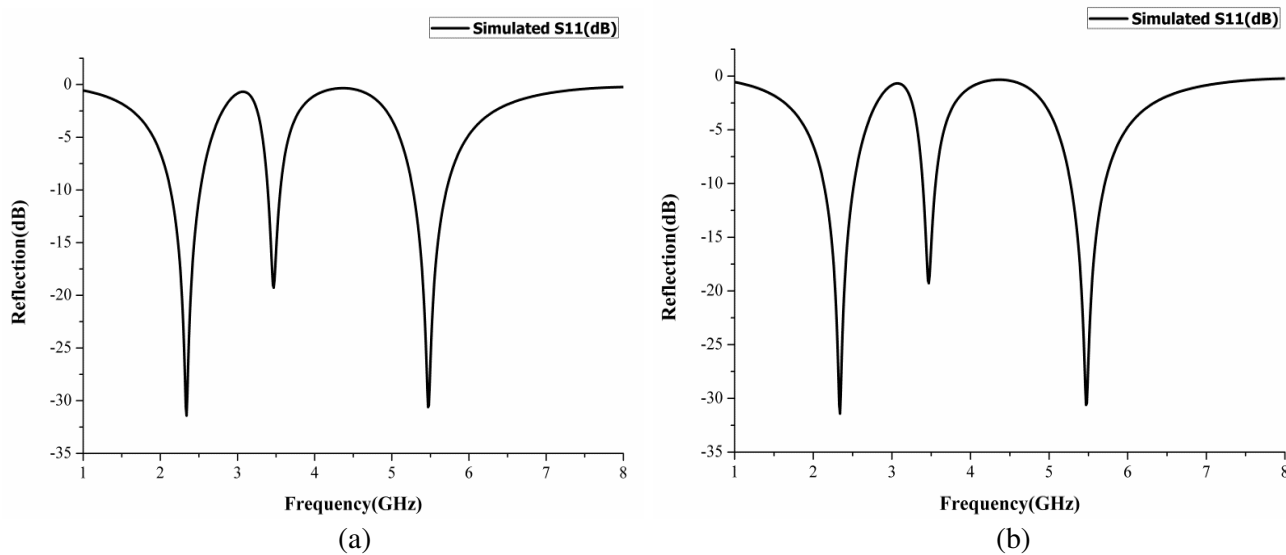


**Figure 5.** Simulated reflection coefficients of proposed unit cell for (a) TE mode, (b) TM mode.

The performance of FSS is measured inside an anechoic chamber by selecting frequencies from 1 GHz to 8 GHz. The proposed structure is mounted on a rotatable table to measure the angular performance. The distance between the two horn antennas remains fixed during the complete measurement.

### 4.3. Measured Results

The measured response of proposed FSS in terms of transmission and reflection coefficients is shown in Figs. 8 and 9, respectively. The measured response is compared with the simulated one for TE mode where the tangential component of electric field is zero in  $z$ -direction. Measured results agree well with the simulated ones as shown in Fig. 8. Similarly, the structure is also tested for TM mode where tangential component of magnetic field is zero in  $z$ -direction as shown in Fig. 8(b).

Stability is the behavior of transmission characteristics at different incidence angles. As working in space, the angle of incidence  $\theta$  could strike the FSS at any arbitrary angle, and its frequency

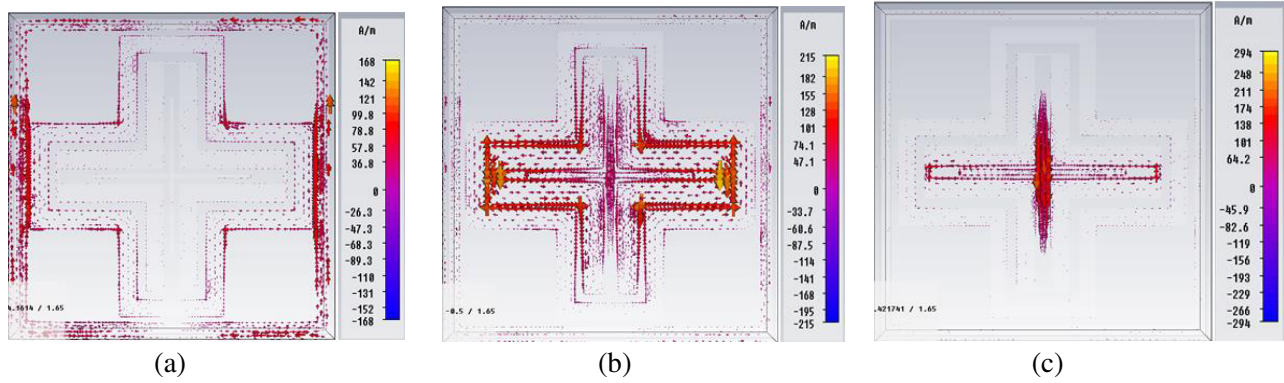


Figure 6. Simulated electric field of proposed unit cell at (a) 2.5 GHz, (b) 3.5 GHz and (c) 5.5 GHz.

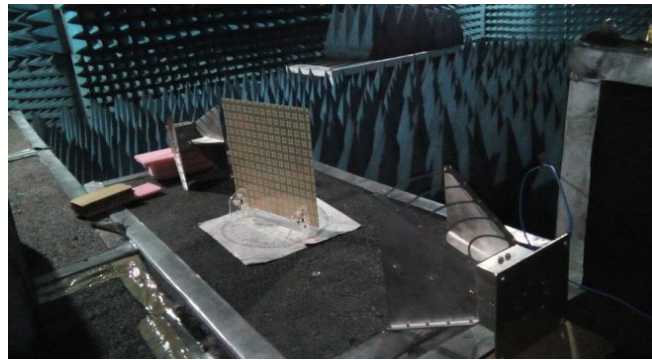


Figure 7. Measurement of FSS under TM mode in an anechoic chamber.

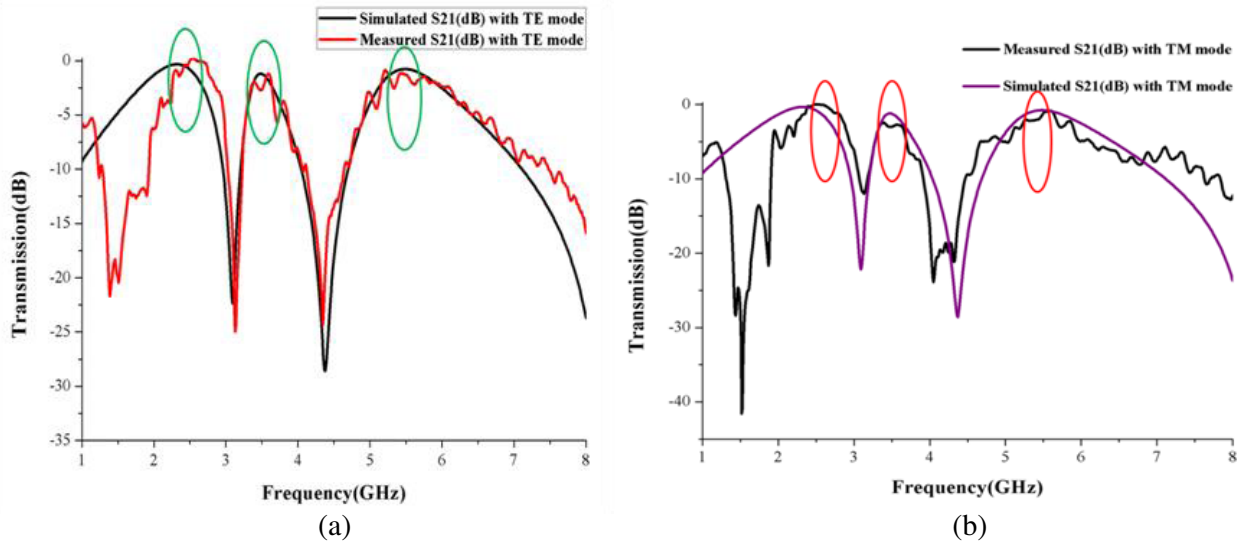
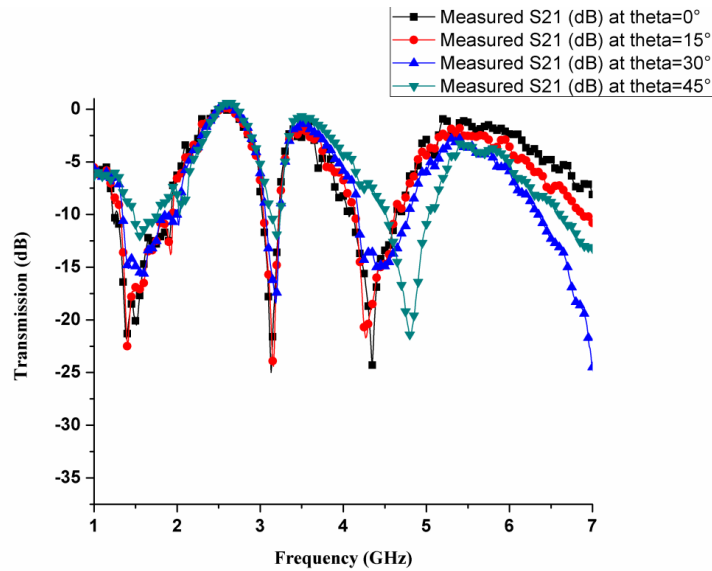
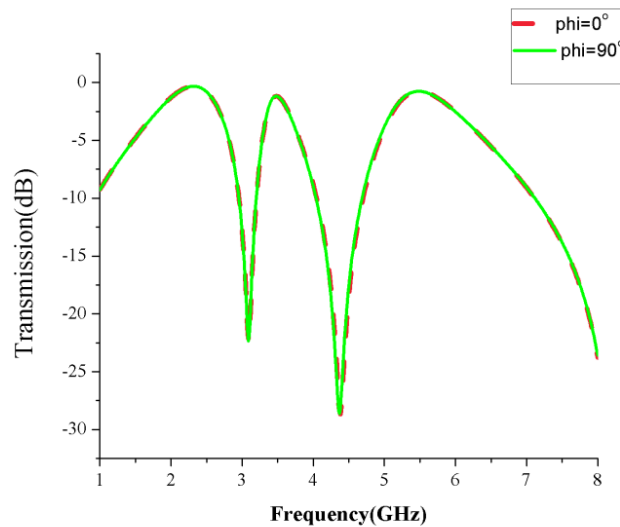


Figure 8. Measured and simulated transmission coefficient of proposed FSS for (a) TE mode, (b) TM mode.

response must be unchanged as theta changes. Measured transmission coefficients are obtained at different values of theta as plotted in Fig. 9. 2.5 GHz band remains the same, and it is irrespective of theta. 3.5 GHz band becomes broader as theta increases while 5.5 GHz band becomes narrower as



**Figure 9.** Transmission coefficients showing variation of incident angles for TE mode.



**Figure 10.** Transmission coefficient of unit cell at different polarization angle phi.

theta increases, but these changes are insignificant. The variation of theta does not shift the resonance frequency of operating bands, hence it can be said that the structure is quite stable with respect to the incidence angle.

While changing the polarization angle phi ( $\Phi$ ) from  $0^\circ$  to  $90^\circ$ , frequency response does not change due to the symmetrical nature of the unit cell as shown in Fig. 10.

As dielectric material FR4 is a lossy material, it absorbs power. Absorption along with the transmission and reflection is plotted in Fig. 11. It can be calculated from Eq. (4),

$$A = 1 - |S_{11}|^2 - |S_{21}|^2 \tag{4}$$

where,

$A$  = Absorption,

$|S_{11}|$  = Linear magnitude of reflection,

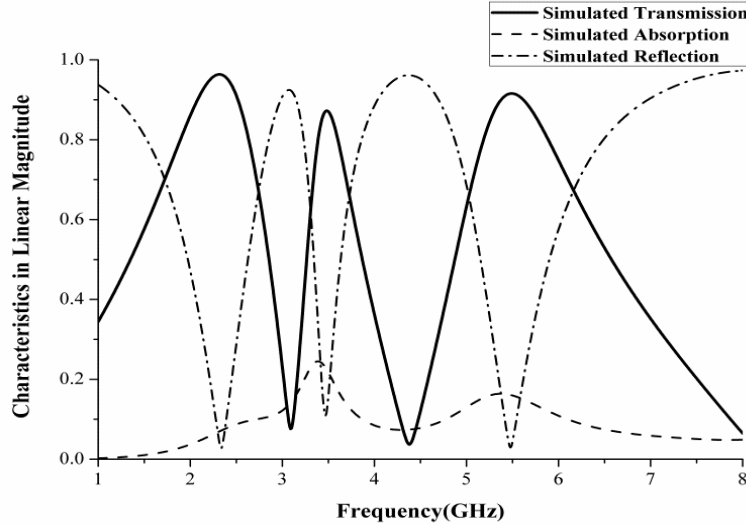


**Figure 11.** Characteristics of FSS: Transmission, reflection and absorption (in linear magnitude).

**Table 3.** Comparison of the performance of proposed structure with previous works.

Reference	Frequency (GHz)	Size of unit cell ( $\lambda^2$ )	No. of operating bands	Type of FSS	Type of Structure	Angular Stability
[6]	8.11, 9.81 and 11	$0.55 \times 0.55$	3	Bandpass	One Sided	NA
[11]	0.621, 0.822 and 0.981	$0.7 \times 0.7$	3	Bandpass	3 Dimention	NA
[17]	2.5	$0.167 \times 0.167$	1	Bandpass	Two Sided	$0^\circ-45^\circ$
[19]	5.72 and 9.79	$0.156 \times 0.14$	2	Bandpass	Two Sided	$0^\circ-30^\circ$
This work	2.6, 3.5 and 5.5	$0.16 \times 0.16$	3	Bandpass	One Sided	$0^\circ-45^\circ$

$|S_{21}|$  = Linear magnitude of transmission.

The performance of the proposed structure is compared with previously reported bandpass structures. Comparison is made in Table 3. After comparing the performance of proposed structure with previously reported works, we can say that the proposed structure is compact in size, and it is a single-layered structure. The orientations of all unit cells are in the same direction. The proposed structure is simple in terms of realization and operates in three different frequency bands. The ratio of the higher to lower resonance frequency is greater than 2.1. It is possible to realize a structure which can have operating bands very distinct from each other, and it can cover wide range of frequencies. The future scope of the proposed work is to realize a structure by integrating FSS with EBG [20, 21].

## 5. CONCLUSION

A novel single layer tri-band bandpass FSS with stable response has been designed for Wi-MAX and WLAN applications. Tri-band bandpass performance is obtained by etching two different metallic loops and one dipole over a low cost FR4 substrate. The stable response is obtained up to  $45^\circ$  angle of incidence for TE and TM modes, and it is achieved due to symmetric nature of the geometry. Approximately, 96%, 87%, and 91% of signal are transmitted at the first, second, and third frequency bands, respectively. A tri-band bandpass characteristic with wide angular stability makes the structure compatible for large range of wireless applications.

## REFERENCES

1. Kushwaha, N., R. Kumar, R. Ram Krishna, and T. Oli, "Design and analysis of new compact UWB frequency selective surface and its equivalent circuit," *Progress In Electromagnetic Research C*, Vol. 46, 31–39, 2014.
2. Munk, B. A., *Frequency Selective Surfaces: Theory and Design*, Wiley-Interscience, New York, 2000.
3. Wu, T. K., *Frequency Selective Surface and Grid Array*, A Wiley Interscience Publication, 1995.
4. Zhou, H., S. Qu, Z. Xu, J. Wang, H. Ma, W. Peng, B. Lin, and P. Bai, "A tri-band second-order frequency selective surface," *IEEE Antennas and Wireless Propagation Letters*, Vol. 10, 507–509, 2011, doi: 10.1109/LAWP.2011.2157074.
5. Yadav, S., C. P. Jain, and M. M. Sharma, "Polarization independent dual-bandpass frequency selective surface for Wi-Max applications," *Int. J. RF Microw. Comput. Aided Eng.*, Vol. 28, No. 6, e21278, August 2018, doi.org/10.1002/mmce.21278.
6. Mahaveer, U., K. T. Chandrasekaran, M. P. Mohan, A. Alphones, M. Y. Siyal, and M. F. Karim, "A tri-band frequency-selective surface," *Journal of Electromagnetic Waves and Applications*, Vol. 35, No. 7, 861–873, 2021, doi: 10.1080/09205071.2020.1865206.
7. Chen, H.-Y. and Y. Tao, "Bandwidth enhancement of a U-slot patch antenna using dual-band frequency-selective surface with double rectangular ring elements," *Microw. Opt. Technol. Lett.*, Vol. 53, No. 7, 1547–1553, 2011, doi: 10.1002/mop.26066.
8. Ditti, S. K. and S. Das, "On a polarization-independent frequency-selective surface (FSS)," *Microw. Opt. Technol. Lett.*, Vol. 44, 249–250, 2005, doi: 10.1002/mop.20601.
9. Ramaccia, D., A. Toscano, A. Colasante, G. Bellaveglia, and R. Lo Forti, "Inductive tri-band double element FSS for space applications," *Progress In Electromagnetics Research C*, Vol. 18, 87–101, 2011.
10. Sivasamy, R. and M. Kanagasabai, "A novel dual-band angular independent FSS with closely spaced frequency response," *IEEE Microwave and Wireless Components Letters*, Vol. 25, No. 5, 298–300, 2015, doi: 10.1109/LMWC.2015.2410591.
11. Lu, Z. H., P. G. Liu, and X. J. Huang, "A novel three-dimensional frequency selective structure," *IEEE Antennas and Wireless Propagation Letters*, Vol. 11, 588–591, 2012, doi: 10.1109/LAWP.2012.2201438.
12. Qing, A. and C. K. Lee, *Differential Evolution in Electromagnetic*, Springer-Verlag, Heidelberg, Berlin, 2010.
13. Islam, S., J. Stiens, G. Poesen, I. Jaeger, W. De Raedt, and R. Vounckx, "Heuristic approach of finite grounded frequency selective surface arrays characterization in W-band," *Proceedings Symposium IEEE/LEOS Benelux Chapter*, Twente, 2008.
14. Narayan, S., B. Sangeetha, and R. M. Jha, *Frequency Selective Surfaces Based High Performance Microstrip Antenna*, Springer, Singapore, 2016.
15. Yadav, S., C. P. Jain, and M. M. Sharma, "Smartphone frequency shielding with penta-bandstop FSS for security and electromagnetic health applications," *IEEE Transactions on Electromagnetic Compatibility*, Vol. 61, No. 3, 887–892, June 2019, doi: 10.1109/TEMC.2018.2839707.
16. Ibrahimi, A., S. Nirantar, W. Withayachumnankul, M. Bhaskaran, S. Sriram, S. F. Al-Sarawi and D. Abbott, "Second-order tetrahertz band pass frequency selective surface with miniaturized elements," *IEEE Transaction on Tetrahertz Science and Technology*, Vol. 5, 2015, doi: 10.1109/TTHZ.2015.2452813.
17. Yadav, S., B. Peswani, R. Choudhury, and M. M. Sharma, "Miniaturized band pass double-layered frequency selective superstrate for Wi-Max applications," *2014 IEEE Symposium on Wireless Technology and Applications (ISWTA)*, 182–187, 2014, doi: 10.1109/ISWTA.2014.6981183.
18. Katoch, K., N. Jaglan, and S. D. Gupta, "Design of a triple band notched compact FSS at UWB. frequency range," *Progress In Electromagnetic Research M*, Vol. 87, 147–157, 2019.

19. Lee, I.-G., Y. B. Park, H.-J. Chun, Y.-J. Kim, and I.-P. Hong, "Design of active frequency selective surface with curved composite structures and tunable frequency response," *International Journal of Antennas and Propagation*, Vol. 2017, Article ID 6307528, 1–10, doi: 10.1155/2017/6307528.
20. Huang, C., C. Ji, X. Wu, J. Song, and X. Luo, "Combining FSS and EBG surfaces for high-efficiency transmission and low-scattering properties," *IEEE Transactions on Antennas and Propagation*, Vol. 66, No. 3, 1628–1632, March 2018, doi: 10.1109/TAP.2018.2790430.
21. Annam, K., S. Kumar Khah, S. Dooley, C. Cerny, and G. Subramanyam, "Experimental design of bandstop filters based on unconventional defected ground structures," *Microw. Opt. Technol. Lett.*, Vol. 58, 2969–2973, 2016, doi: 10.1002/mop.30192.